Status report: Characterization of Weld Residual Stresses on a Full-Diameter SNF Interim Storage Canister Mockup

Fuel Cycle Research & Development

Prepared for
U.S. Department of Energy
Used Fuel Disposition Program

D.G. Enos and C.R. Bryan
Sandia National Laboratories

August 21, 2015

FCRD-UFD-2015-00123
SAND2015-7068 R

Sandia National Laboratories is a multi-program laboratory managed and operated by Sandia Corporation, a wholly owned subsidiary of Lockheed Martin Corporation, for the U.S. Department of Energy's National Nuclear Security Administration under contract DE-AC04-94AL85000.

APPENDIX E
FCT DOCUMENT COVER SHEET [1]

Name/Title of Deliverable/Milestone/Revision No.	Status report: Characterization of Weld Residual Stresses on a Full-Diameter SNF Interim Storage Canister Mockup
Work Package Title and Number	ST Storage and Transportation Experiments - SNL FT-15SN080505 (Rev. 2)
Work Package WBS Number	1.02.08.05
Responsible Work Package Manager	Charles R. Bryan / Charles R. Bryan (Name/Signature) August 21, 2014 Date Submitted

Quality Rigor Level for Deliverable/Milestone[2]	☒ QRL-3	☐ QRL-2	☐ QRL-1 Nuclear Data	☐ Lab/Participant QA Program (no additional FCT QA requirements)

This deliverable was prepared in accordance with Sandia National Laboratories
(Participant/National Laboratory Name)

QA program which meets the requirements of

☒ DOE Order 414.1 ☐ NQA-1-2000 ☒ Other: FCT QAPD

This Deliverable was subjected to:

☒ Technical Review ☐ Peer Review

Technical Review (TR)
Review Documentation Provided

☐ Signed TR Report or,
☐ Signed TR Concurrence Sheet or,
☒ Signature of TR Reviewer(s) below

Peer Review (PR)
Review Documentation Provided

☐ Signed PR Report or,
☐ Signed PR Concurrence Sheet or,
☐ Signature of PR Reviewer(s) below

Name and Signature of Reviewers

Jeff Rodelas

Don Susan

NOTE 1: *Appendix E should be filled out and submitted with the deliverable. Or, if the PICS:NE system permits, completely enter all applicable information in the PICS:NE Deliverable Form. The requirement is to ensure that all applicable information is entered either in the PICS:NE system or by using the FCT Document Cover Sheet.*

NOTE 2: *In some cases there may be a milestone where an item is being fabricated, maintenance is being performed on a facility, or a document is being issued through a formal document control process where it specifically calls out a formal review of the document. In these cases, documentation (e.g., inspection report, maintenance request, work planning package documentation or the documented review of the issued document through the document control process) of the completion of the activity, along with the Document Cover Sheet, is sufficient to demonstrate achieving the milestone. If QRL 1, 2, or 3 is not assigned, then the Lab / Participant QA Program (no additional FCT QA requirements) box must be checked, and the work is understood to be performed and any deliverable developed in conformance with the respective National Laboratory / Participant, DOE or NNSA-approved QA Program.*

SUMMARY

Stress corrosion cracking (SCC) of interim storage containers has been indicated as a high priority data gap by the Department of Energy (Hanson et al. 2012), the Electric Power Research Institute (EPRI 2011), the Nuclear Waste Technical Review Board (NWTRB 2010a), and the Nuclear Regulatory Commission (NRC 2012a; 2012b). Uncertainties exist both in terms of the environmental conditions that prevail on the surface of the storage containers and the electrochemical properties of the storage containers themselves. The goal of the work described in this document is to assess the effects of the manufacturing process on canister performance by evaluating the properties of a full-diameter cylindrical mockup of an interim storage canister. This mockup has been produced using the same manufacturing procedures as fielded spent nuclear fuel interim storage canisters. This document describes the design and procurement of the mockup and the planned characterization work. It also provides the status of the project, describing the cutting of the mockup into sections for different analyses, and presenting initial results from the stress characterization effort.

In order for SCC to be a viable degradation mode, three criteria must be met – there must be a sufficiently large stress in the material to support crack growth, the material itself must be susceptible to stress corrosion cracking, and the environment must be sufficiently aggressive to support crack initiation and propagation. The work described in this document is aimed at evaluating the first two of these criteria for in-service containers by characterizing the material properties of the base metal and weld zones on the canister mockup. Assessment of residual stresses associated with forming and welding was performed using a combination of three techniques. These include deep-hole drilling, the contour method, and x-ray diffraction. The deep-hole drilling technique allows measurement of residual stresses along a one-dimensional hole drilled through the wall of the cylinder; it allows measurement of stresses within the intact cylinder and hence, captures the effects of the cylindrical constraint on the stresses. The contour method provides a two-dimensional map of stresses along a cross section through a region of interest; however, the mockup must be cut into pieces to measure the face of the cross section, and stresses due to the constraint of the intact cylinder are lost. X-ray diffraction allows assessment of very shallow near-surface stresses, and potentially phase changes (e.g., formation of deformation-induced martensite), associated with shaping and grinding the mockup. It is also used to map stress components that are in-plane with the cross sectional surface, when using the contour method.

Characterization of residual stresses in the mockup has begun. After fabrication, the mockup was cut into three sections. The largest section was reserved for residual stress measurements; the other two pieces will be used for material characterization studies and testing of SCC evaluation methods. During the cutting process, strain gauges were used to monitor stress relaxation at locations where weld residual stresses will ultimately be measured, so that it can be added back in if necessary to obtain the as-manufactured residual stresses. However, measured strains were very small, and can be ignored; cutting the cylinder in half had little effect on residual stresses. One set of stress measurements has been collected to date, at a base metal location far from any weld. The incremental center-hole drilling technique was used to measure very shallow stresses (<0.5 mm), while the incremental deep-hole drilling technique was used to measure the through-thickness stress profile. Results indicate that in this non-welded region, residual stresses are dominated by those introduced during the forming of the plate to make a cylinder. The rolling process extended the outer surface of the shell while shortening the inner surface, and the residual stresses reflect this; except for near-surface regions, the other half of the shell wall is under

tension, while the inner half of the wall is under compression. These data will provide a baseline for the residual stresses near the weld zones, to be measured in coming months.

Evaluation of the electrochemical properties of the welded regions of the container will first involve an assessment of the microstructure of the regions at the longitudinal, circumferential, and repair welds via standard metallurgical techniques. The thermal cycling associated with the welding process will, in addition to altering the overall microstructure of the near-weld material, result in the precipitation of chromium carbides and the formation of chromium-depleted regions along the grain boundaries. This effect, known as sensitization, will be particularly pronounced in the weld heat affected zone (i.e., the region near the weld fusion zone that has been impacted by the heat input from the welding process). The extent to which sensitization has taken place will be documented as a function of position from the edge of the weld fusion zone. This will be done both for the near-surface regions and through the thickness of the container wall. A volumetric assessment of the degree of sensitization will illustrate the extent of the affected region and illustrate the presence/absence of an active path for crack propagation through the material.

Establishing the storage canister susceptibility to SCC will require both the crack nucleation and crack propagation processes be assessed using samples with relevant crystallographic textures and electrochemical properties, under typical environmental conditions under stress conditions as defined by analyses of the full scale mock-up. A variety of experiments are planned to evaluate both aspects of the cracking process, as well as to define methods to produce relevant weld analog materials.

Upon completion of the residual stress measurements, the mock-up will be sectioned to provide samples for stress corrosion cracking initiation tests. These coupons are critical for the UFD program, but also are of great interest to outside parties such as EPRI and the academic groups working on canister SCC as part of the DOE NEUP programs. Samples will be disseminated to interested parties on an as-needed basis, with the UFD program getting first priority, followed by the DOE-funded NEUP groups and EPRI.

CONTENTS

FIGURES

TABLES

ACRONYMS

ASME B&PVC	American Society of Mechanical Engineers Boiler and Pressure Vessel Code
ASTM	American Society for Testing and Materials
CISCC	Chloride Induced Stress Corrosion Cracking
DHD	Deep Hole Drilling
DOE	Department of Energy
EDM	Electric Discharge Machining
EPR	Electrochemical Reactivation
EPRI	Electric Power Research Institute
FCRD	Fuel Cycle Research and Development
HAZ	Heat-Affected Zone
iCHD	Incremental Center-Hole Drilling
iDHD	Incremental Deep-Hole Drilling
ISFSI	Independent Spent Fuel Storage Installation
LANSCE	Los Alamos Neutron Science Center
NDE	Non-Destructive Evaluation
NEUP	Nuclear Energy University Programs
NRC	Nuclear Regulatory Commission
NWTRB	Nuclear Waste Technical Review Board
QA	Quality Assurance
SCC	Stress Corrosion Cracking
SNF	Spent Nuclear Fuel
SS	Stainless Steel
UFD	Used Fuel Disposition
WRS	Weld Residual Stress
XRD	X-Ray Diffraction

STATUS REPORT:

CHARACTERIZATION OF WELD RESIDUAL STRESSES ON A FULL-DIAMETER SNF INTERIM STORAGE CANISTER MOCKUP

1. INTRODUCTION

The potential for stress corrosion cracking (SCC) of welded stainless steel interim storage containers for spent nuclear fuel (SNF) has been identified as a high priority data gap by the Nuclear Waste Technical Review Board (NWTRB 2010b), the Electric Power Research Institute (EPRI 2011), the Department of Energy (DOE) Fuel Cycle Research and Development (FCRD) programs Used Fuel Disposition (UFD) campaign (Hanson et al. 2012), and the Nuclear Regulatory Commission (NRC 2012a; 2012b). Uncertainties exist both in the understanding of the environmental conditions on the surface of the storage canisters and in the textural, microstructural, and electrochemical properties of the storage containers themselves. The canister surface environment is currently being evaluated by Sandia and EPRI (Enos et al. 2013; Bryan and Enos 2014; EPRI 2014; Bryan and Enos 2015); however, little has been done to assess canister material properties and their impact on corrosion. Of specific interest are weld zones on the canisters, because the welding process modifies the microstructure of the stainless steel as well as its resistance to localized corrosion. In addition, welding introduces high tensile residual stresses that can drive the initiation and growth of SCC cracks. In order to meet the need for additional data on the canister material properties, the UFD campaign has procured a full-diameter cylindrical mockup of a dual certified 304/304L stainless steel (SS) storage canister produced using the same manufacturing procedures as fielded SNF fuel interim storage canisters. The weld and base metal zones on this mockup will be characterized to determine metal properties and susceptibility to SCC. This report documents the mockup specifications and manufacturing processes; the initial cutting of the mockup into three cylindrical pieces for testing and the measured strain changes that occurred during the cutting process; and the planned weld residual stress characterization activities and the status of those activities.

Section 2 of this report provides background on the issue of SCC of interim storage canisters and describes the necessary criteria for SCC to occur, in the context of providing rationale for the purchase and analysis of the mockup. Section 3 describes the material, design, quality assurance (QA) specifications, and procurement of the mockup. Section 4 summarizes the planned characterization activities, which are described in detail in the document *Technical Work Plan: Characterization of Weld Regions on a Full-Scale Cylindrical Mockup of an Interim Storage Container*, FCRD-UFD-2014-000710 (Enos and Bryan 2014). Section 5 provides the current status of the characterization work, and describes the cutting of the mockup, the results of strain measurements performed during the cutting process to monitor relaxation due to cutting, and the results of initial stress measurements on the mockup. Finally, Section 6 provides a preliminary schedule for the rest of the planned analyses.

2. BACKGROUND

Following initial cooling in pools, SNF is transferred to dry storage casks for longer-term storage at the reactor sites. The storage cask systems are predominantly welded stainless steel (Hanson et al. 2012) containers enclosed within a ventilated concrete or steel overpack. These cask systems are intended as interim storage until a permanent disposal site is developed, and until recently, were licensed for up to 20 years, and renewals also up to 20 years. In 2011, 10 CFR 72.42(a) was modified to allow for initial license periods of up to 40 years, and also, license extensions of up to 40 years. However, as the United States does not currently have a final disposal pathway for SNF, these containers may be required to

perform their waste isolation function for many decades beyond the original design intent. As noted above, several recent analyses (NWTRB 2010b; EPRI 2011; Hanson et al. 2012; NRC 2012a) have identified and prioritized potential concerns with respect to the safety performance of long-term interim storage. In each of these studies, the potential for canister failure by chloride-induced SCC (CISCC) was identified as the major concern with respect to canister performance.

2.1 Criteria for Stress Corrosion Cracking

Stress corrosion cracking is a localized corrosion phenomenon by which a through-wall crack could potentially form in a canister outer wall over time intervals that are shorter than possible dry storage times. In order for SCC to occur, three criteria must be met (Figure 1): an aggressive chemical environment must exist, the metal must be susceptible to SCC, and sufficient tensile stress must be present to support SCC. In general, these criteria are expected to be met, at least at some Independent Spent Fuel Storage Installation (ISFSI) sites, during the period of interim storage.

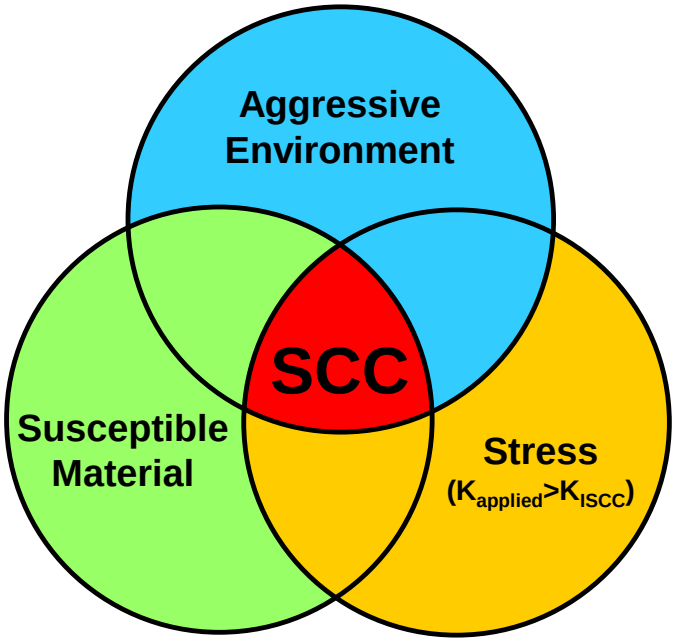

Figure 1: Criteria for SCC initiation and propagation.

Aggressive chemical environment: Field sampling of surface deposits on in-service SNF storage canisters at three near-marine ISFSI sites has been carried out over the last three years, and analyses have shown that chloride-rich salts can be present on the canister surfaces (Enos et al. 2013; Bryan and Enos 2014; EPRI 2014; Bryan and Enos 2015). Once portions of the canister surfaces cool sufficiently for these salts to deliquesce, a corrosive chloride-rich aqueous environment could potentially form.

Susceptible material: The majority of SNF dry storage casks currently in use are made from austenitic stainless steels, including 304, 304L, and 316. Should sufficient tensile stress be present, there is ample evidence that these stainless steels are susceptible to CISCC in aggressive chloride-bearing environments. SCC of 304 SS, the most widely used alloy for containers that are currently in service, occurs readily in experimental tests with deliquesced sea-salts (e.g., (Nakayama 2006; Prosek et al. 2009; Tani et al. 2009; Mintz et al. 2012; Prosek et al. 2014), and has also been observed in near-marine ambient temperature

field tests and industrial sites (Kain 1990; Hayashibara et al. 2008; Kosaki 2008; Cook et al. 2011; Nakayama and Sakakibara 2013; Cook et al. 2014). However, overall susceptibility is a function of several factors, including the degree of sensitization, the degree of cold work, and the surface finish (Parrott and Pitts 2011); to date, none of these factors have been assessed for materials representative of fielded interim storage canisters.

- Degree of sensitization — austenitic stainless steels contain a small amount of carbon, and are prone to a phenomenon known as sensitization when welded. In the material adjacent to the weld fusion zone (i.e., the heat affected zone (HAZ)) the thermal cycling associated with the welding process facilitates the nucleation of chromium carbides along grain boundaries. The diffusion of chromium from the surrounding microstructure enables growth of these carbides. As the mass transfer rate of chromium is much higher along grain boundaries than in the bulk of the material, chromium moves from the material within each grain to the grain boundary, where it rapidly diffuses to the growing chromium carbides. As a result, the regions adjacent to the grain boundaries become depleted in chromium, eventually dropping to well below the 10% Cr threshold required to maintain a protective chromium oxide on the metal surface. These Cr-depleted zones are thus more susceptible to corrosion than the surrounding grains, and serve as a preferential site for localized corrosion initiation. These localized corrosion sites, in turn, can serve as initiation sites for stress corrosion cracking. The first grain boundaries to become sensitized are those along which there is the greatest lattice mismatch between adjacent grains, but with progressive heating, more and more grain boundaries become sensitized. The degree of sensitization is defined as the percentage of grain boundaries that are sensitized. In general, the degree of sensitization induced by welding increases with the thickness of the weld, as the heat input is greater.

  Sensitization has many effects on localized corrosion. As the degree of sensitization increases, pit incubation times decrease, while pit nucleation and growth rates increase. As pits frequently serve as initiation sites for SCC, the nucleation rate for SCC cracks also increases. Nakayama and Sakakibara (2013) estimate that the induction time for SCC initiation can decrease by more than an order of magnitude as the degree of sensitization increases from 0 to 20%, and that crack propagation rates can increase by a factor of 5, for atmospheric SCC conditions. Khatak et al. (1996) also saw increases in crack growth rates for sensitized 304 SS, and noted that sensitization significantly lowered the threshold stress intensity for SCC. Sensitization can also result in a change in the SCC mechanism: in sensitized materials SCC is, at least initially, intergranular, while in unsensitized materials, it is transgranular.

  The degree to which an austenitic stainless steel can sensitize is a function of its carbon content, with reduced carbon content alloys (e.g., L grade stainless steels such as 304L) being less susceptible. Current canisters are made from dual-certified 304/304L SS; however, some early canisters may have been made from 304 SS with a higher carbon content (Pacific Nuclear Fuel Services 1991).

- Degree of cold work — The deformation of concern here comes from two sources – the bending of the plate stock used to manufacture the container into a cylinder, as well as local deformation due to grinding operations on the surface of the container, with the magnitude of the latter being the most significant. Cold work can adversely affect the corrosion resistance of stainless steels (Khatak et al. 1996; García et al. 2001; Parrott and Pitts 2011). First, it results in the formation of extensive dislocation structures within the metal matrix, which can result in the formation of regions where destabilization of the protective oxide layer is more likely and the ability of the material to repassivate is degraded (Peguet et al. 2007), increasing the susceptibility to localized attack. For large deformation, the formation of strain-induced martensite in the metal is possible, which is less resistant to corrosion than austenite. Martensite that is incident with the metal surface can serve as sites where the susceptibility to localized corrosion initiation is enhanced. SCC crack growth rates have also been observed to increase with increasing cold work, particularly at 20% cold work and above (Kuniya et al. 1988).

- Surface finish — A rough surface finish (>1 μm) has also been found to promote initiation of localized corrosion, as chloride ions are trapped and concentrated in heterogeneities that exist on the metal surface (Parrott and Pitts 2011). Surface grinding can also produce large local variations in stress and microstructure near the surface, which may contribute by increasing strain energy and the dissolution rate of the metal (Ghosh and Kain 2010a; 2010b; Ghosh et al. 2011). Localized corrosion initiation at the highly stressed surface irregularities also results in an increased nucleation rate of SCC cracks within and adjacent to the resulting pits (Turnbull et al. 2011). All storage canisters will have a roughly ground surface with a roughness well in excess of 1 μm.

While these factors are known to affect susceptibility to SCC, they are all specific to the material and to the manufacturing processes used to fabricate the canister. In order to evaluate them, it is necessary to obtain relevant metal samples, from a canister or mockup made using the same techniques as real, in-service canisters.

Tensile stress: In order for an SCC crack to initiate, the tensile stresses in the metal must be of a sufficiently large magnitude that the threshold stress intensity value at a potential nucleation site is exceeded. In order for an initiated crack to propagate and penetrate through the container, the applied stress intensity at the crack front must be maintained above that threshold. In other words, a sufficiently large tensile stress state must exist through the entire wall thickness. Tensile stresses may be applied externally—for instance, by loading or by pressurization—but for SNF interim fuel canisters, external loads are negligible relative to the yield stress of the metal. High residual tensile stresses may be present in the metal, however, due to cold working or welding. Weld residual stresses (WRS) are generally the most important component, and are a function of many factors, including weld geometry, sample thickness, welding speed, number of passes, inter-pass temperatures, and base metal properties relative to the weld. Because of this, WRS are specific to the geometry and welding processes used, and can only be measured from an actual storage canister or a mockup made using the same procedures as the real canisters. However, WRS measurements on samples with relevant geometries and typical welds have never been done. The NRC modeled WRS for typical canister welds using finite element methods (NRC 2013), and predicted that within the HAZ of both longitudinal and circumferential welds, sufficient tensile stresses would be present to support SCC. Moreover, they predicted that the tensile stresses would be present through the thickness of the cylinder wall, permitting full penetration over time.

2.2 Need for a Full-Sized Mockup

The DOE has recognized that evaluation of the material susceptibility and weld residual stresses in interim storage canisters is critical to understanding the implications of the potentially corrosive environment that may develop on the surface of the canisters. These material properties control the likelihood of SCC initiation, and ultimately, the rate at which any nucleated crack will grow should SCC develop, along with the potential for crack stifling prior to penetration. For this reason, the DOE has purchased a full-diameter cylindrical mockup, made using materials and manufacturing procedures identical to those used to fabricate one particular in-service storage canister design. The canister mockup will be characterized using a suite of different techniques, as described in the following sections, with the goal of determining the following:

1. The near-surface and through-thickness residual stress states associated with the welds used to construct the container
2. Stress states near weld repair zones, synthetically introduced to the mockup.
3. The near-surface and through-thickness residual stress states associated with the as-formed walls of the container (i.e., far from the welds)
4. The degree of sensitization associated with the various weldments used to form the container

5. Textural and metallurgical characteristics of the welds and HAZ, and changes in the near-surface metal of the canister shell due to cold-working, and their potential impact on the corrosion properties of the metal.

3. DESIGN AND PROCUREMENT

The material properties that will be measured are strongly controlled by the materials and manufacturing processes used to make the interim storage canister. Therefore, the mockup had to be made using the same materials and fabrication methods as a real canister. Nearly all storage canister designs use 304 SS (for older containers) and welding is multi-pass, predominantly utilizing the submerged arc welding process with a double-V edge preparation. To ensure consistency with a real canister design, price quotations were requested from the three major cask vendors. Areva/TN (formerly TransNuclear) makes horizontal canister storage systems, and their NUHOMS systems account for about 37% of all storage systems presently deployed in the US. HOLTEC International and NAC International manufacture vertical canister storage systems, and account for about 32% and 19% of all current canister systems, respectively. However, HOLTEC and NAC did not submit a bid. Areva/TN did not respond directly, but instead recommended that Ranor Inc. be contacted. Ranor is an industrial manufacturing/fabrication facility that in the past has been contracted to build stainless steel storage canisters for TransNuclear. With the permission of Areva/TN, Ranor was willing to build the mockup using identical materials and procedures as were used to build the original TransNuclear horizontal storage canisters. Ranor was ultimately contracted to build the mockup.

The mock-up whose evaluation is described in this document is based upon the TransNuclear NUHOMS 24P design (Pacific Nuclear Fuel Services 1991). This container design is employed at the Calvert Cliffs nuclear power station, which was the first site surveyed by EPRI for the dust composition on the surface of the containers (Gellrich 2013). The mock-up, pictured schematically in Figure 2 below, consists of three cylindrical shells, each being 48 inches long and 67.2 inches in diameter, and having a wall thickness of 5/8 inch. Each shell was formed by cold forming a plate into a cylinder, then making a single longitudinal weld to form the cylinder. The three cylinders were then welded together to form a single large cylinder 12 feet in length with two circumferential welds. All of the welds were formed via the submerged-arc welding process and were multi-pass. Each inner-diameter weld consisted of three passes, and with one exception, each outer-diameter weld was made with four passes (the exception had 5). The inner diameter was welded first, followed by the outer diameter. Welds were made at a rate of 15 to 16 inches per minute at a voltage of 30V and current of 400A. Typical heat input was 45 kJ/in.

In addition to welds formed under nominal conditions, discussions with TransNuclear and Holtec have indicated that during construction of actual storage containers, repairs are commonly necessary at regions along the welds where the nondestructive testing indicated that the weld did not conform to the criteria in ASME B&PVC Section III, Division 1, Subsection NB. Repair regions have been identified by numerous researchers as having dramatically elevated residual stresses when compared to unrepaired portions of a weld (Dong et al. 2002; Bouchard et al. 2005; Dong et al. 2005; Elcoate et al. 2005; George and Smith 2005; Hossain et al. 2006; Hossain et al. 2011). During fabrication of the mockup, all of the welds were subjected to a full radiographic inspection, and no weld repairs were required. However, because of the potentially important effect of weld repairs on weld residual stresses and material properties, one region on each circumferential weld was subjected to a repair procedure on the outer diameter. In these locations, the weld metal was removed locally by grinding, then that section rewelded. The repair was welded using the gas tungsten arc welding technique. Characterization of these sites will allow determination of weld residual stresses and degrees of sensitization typical of weld repair regions.

Production of the container was done at Ranor (located in Westminster, MA), the fabrication facility where the containers located at the Calvert Cliffs site were produced. Use of the same manufacturer was critical as, while the overall design is owned by Areva-TN, the production methodologies used are

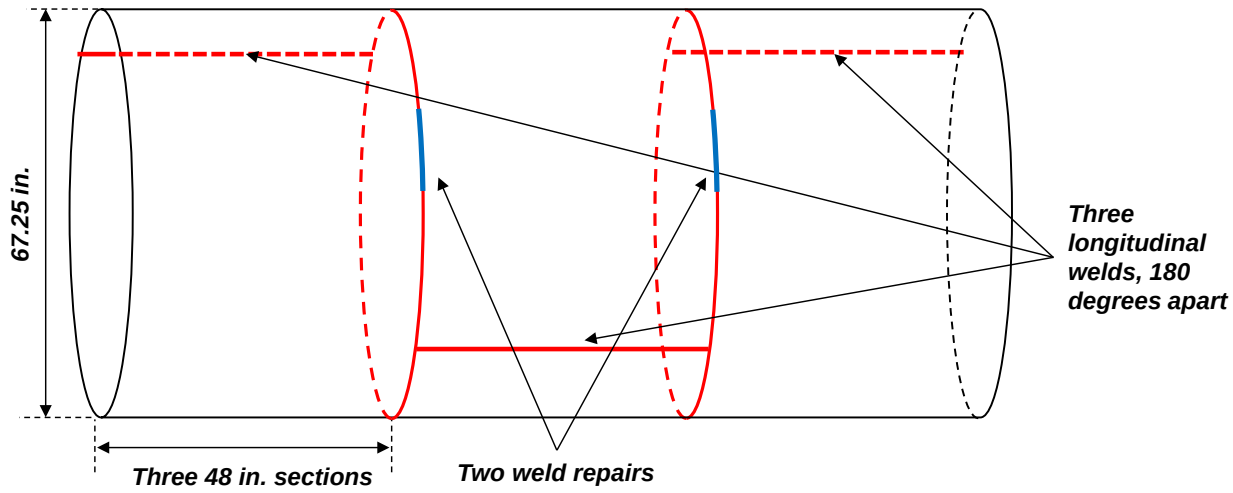

Figure 2: Schematic representation of the full scale mock storage container manufactured at Ranor

proprietary to Ranor. That is, Areva-TN specified the overall design (i.e., material, overall dimensions, etc.) but Ranor developed the methodology to actually build each storage container.

Three plates of dual-certified 304/304L stainless steel were used to construct the container. The thickness of each plate was verified via ultrasonic inspection prior to being welded. The weld filler metal was 308L SS, as typically used when welding 304. The compositions of the 304/304L plates and the 308L filler material are in Table 1 below, and indicate carbon contents below 0.03, meeting the "L" designation. In addition to the composition of the materials of construction, the parameters for each weld pass were documented in the data package provided with the mockup. These include the current, voltage, travel speed, heat input, and interpass temperature. All welds used a double-V edge preparation with a 30 degree bevel. X-ray films of all welds and weld repairs were also included in the data package.

Table 1: Composition of 304L Plate and 308L Filler Metal Used to Construct Mock-Up

	C	Co	Cr	Cu	Mn	Mo	N	Ni	P	S	Si
Plate Material (304/304L)	0.0223	0.1865	18.1000	0.4225	1.7125	0.3180	0.0787	8.0270	0.0305	0.0023	0.2550
Weld Filler (308L) (lot 1)	0.014	--	19.66	0.16	1.70	0.11	0.058	9.56	0.025	0.010	0.39
Weld Filler (308L) (lot 2)	0.012	--	19.71	0.192	1.730	0.071	0.053	9.750	0.024	0.012	0.368

4. PLANNED CHARACTERIZATION ACTIVITIES

4.1 Weld Residual Stress

In addition to a susceptible material and a sufficiently aggressive environment, the nucleation and growth of a stress corrosion crack requires the presence of a sufficiently large stress. In the case of interim storage containers, the stress existing within the structure will predominantly be residual stresses resulting from the forming of the metal plates into a cylinder and the subsequent welding and associated solidification shrinkage of the fusion zone upon cooling.. The latter are likely to be the largest in magnitude, and are the result of the constraint placed by the structure of the container (and any additional fixtures used during fabrication) on the weld as it solidifies. A wide variety of methods are available for residual stress measurement, as summarized in NUREG-2162 (Benson et al. 2014). Techniques are typically based on measurement of elastic strains in the crystal structure using diffraction of either x-rays or neutrons, or on strain measurements made upon mechanically altering the material being investigated (allowing stress relaxation to occur). The techniques vary in terms of their sensitivity and depth of penetration into the substrate metal. The most appropriate technique for assessing the mock-up storage container is one capable of measuring the stresses through the thickness of the container wall. Furthermore, the technique must allow for evaluation of large sections, as it is desired that the stress state be measured prior to and following the sectioning of the container into smaller samples for use in corrosion or stress corrosion cracking experiments.

Three techniques have been initially targeted for use in this study. These include neutron diffraction, the contour method, and the deep-hole drilling method. Neutron diffraction will be explored via collaboration with LANL. The other two techniques will also involve collaboration with other groups capable of performing these measurements.

4.1.1 Deep Hole Drilling

A variety of hole-drilling based techniques are available for the evaluation of the stress state in a metal sample. Typically, these techniques involve the attachment of strain gauges to the surface of the material being measured, which are monitored while a hole is precisely drilled in the material. As the hole is drilled in depth increments, the local constraint within the structure is relaxed, allowing stress relaxation to occur, resulting in surface deformation which is captured by the strain gauges. This method is known as incremental center-hole drilling (iCHD). A similar drilling technique involves the use of a surface strain gauge around which a core is cut into the material, allowing the center pillar to relax. These techniques, while they can be accurate, are only sensitive to the near-surface stresses in the material.

The deep hole drilling methodology differs from other hole-drilling techniques in that it does not rely on the use of surface strain gauges. A small diameter hole is precisely drilled via a gun drill through the material. An air gauge is then used to precisely characterize the diameter of the hole along its length. Next, electric discharge machining (EDM) is used to cut an overcore around the aforementioned hole. As the core is cut, the constraint placed on the metal immediately adjacent to the central hole is relaxed, resulting in local lateral displacement of the material. The inner diameter of the hole is then re-characterized and the resulting change in diameter, due to the loss of constraint around the hole, is recorded. From these strains, the original residual stress state within the material as a function of depth can be calculated. The deep hole drilling technique is not sensitive to near-surface stresses, and hence is commonly combined with iCHD to obtain a full through-thickness weld residual stress profile, if near-surface stresses are of interest.

The calculations used for standard deep hole drilling are based upon the assumption that the stress relaxation leading to the measured displacements is entirely elastic in nature. When large stresses are present, this is not true, and plastic deformation of the material can result, hindering the ability of the technique to resolve stress. For a heavily constrained weld, such as the circumferential weld on the interim storage containers, it is anticipated that the residual stress levels will be very high – approaching

the yield strength of the material – and as such, the traditional analysis will not work. To compensate for this, the deep hole drilling technique must be modified (Mahmoudi et al. 2009; 2011). In the modified technique, the EDM core is cut in steps. After each step, the inner diameter of the hole is characterized via the air probe. By measuring the deformation of the inner diameter of the hole at the depth of the core cut, the effect of plasticity can be addressed. The resulting residual stress distribution, while being lower in vertical resolution than the traditional measurement, is able to resolve large residual stresses. This modified technique is known as incremental deep hole drilling (iDHD).

The deep hole drilling technique is semi-destructive in nature. The drilling of the hole and the EDM overbore is obviously destructive to that region, but the site is small (1.5mm diameter hole, 6mm diameter overbore), but the remainder of the mockup will be undisturbed. Perhaps more importantly, the deep hole drilling technique can be employed without cutting the mock-up into smaller pieces. The contour method, described below, analyzes a cross-sectional surface of the metal, which requires cutting a section of the weld from the mockup. While the use of surface strain gauges can help measure the stress relaxation associated with cutting a section from the mockup, the cutting process introduces an additional level of complexity and adds to the uncertainty of the residual stress measurement.

4.1.2 Contour Method

As with hole drilling techniques, the contour method involves the removal of constraint from the system, and the measurement of the resulting relaxation displacements. In the contour method, the specimen being evaluated is fixtured securely in place, and a cut is made across the region where the stress state is to be assessed. A coordinate measuring machine is then used to precisely measure the deviations of the cut surface resulting from the stress relaxation associated with making the cut. Mathematically, the deviations (i.e., strains) are converted into the residual stress state that existed prior to being cut. In essence, the amount of stress required to force the surface flat is calculated.

The calculated stress field represents one stress direction – perpendicular to the cut surface. In order to get the other two stress directions, X-ray Diffraction (XRD) measurements are made, mapping the other two stress states over the exposed surface.

The contour method is destructive in nature and requires that the region being measured be extracted from the mock-up container. However, the resulting stress distribution is a high resolution map across the entire cut surface. In addition, the use of external strain gauges when extracting the piece of material to be analyzed enables the stress relaxation not captured by the contour measurement itself to be added back in, such that the initial stress state can be accurately estimated. By combining this method with iDHD prior to cutting, changes in stress due to cutting can be even more accurately estimated and corrected for.

4.1.3 Neutron Diffraction

Diffraction-based measurements allow the stress state to be evaluated with little or no cutting of the material being evaluated. The region being analyzed is hit with a collimated beam of neutrons. The neutrons are diffracted from the sample and measured via panel detectors. Using Bragg's law, the diffracted neutrons are used to measure the lattice spacing of the stressed sample. The lattice spacings are then compared to similar measurements taken from an unstressed sample. Based upon the distortion of the stressed sample relative to the unstressed sample, the strain field within the structure can be measured. These strains are then converted to normal stresses through the use of Hooke's law in three dimensions.

By stepping the sample through the neutron beam, the stress distribution in a two-dimensional slice through the sample can be measured. As mentioned above, the use of neutron diffraction requires the availability of an unstressed sample. That sample must have the same metallurgical condition as the region being measured – this includes the microstructure as well as the elemental composition. Deviations in either will add to the uncertainty of the reported stresses. When dealing with specimens that have a uniform structure (chemically and microstructurally) developing the reference sample is relatively straightforward. Unfortunately, in the case of a weld, the structure is extremely non-uniform,

progressing from what may be a uniform grain structure in the bulk metal, to a dendritic structure in the weld fusion zone. As a result, the reference sample must be cut from a segment of the weld nominally identical to that for which the stress state is being analyzed. The reference sample is typically a thin slice, which has been further cut into a comb pattern, relieving any residual stresses within the slice.

Another complication with neutron diffraction is the size of the chamber. There are no chambers available into which the full-scale mockup would fit. The initial test plan (Enos and Bryan 2014) called for cutting a ring from the mockup about 2 feet high, which could be analyzed without further cutting at the Los Alamos Neutron Science Center (LANSCE) at Los Alamos National Laboratory. However, because of funding reductions at LANSCE, it is no longer a user facility and is no longer available. No other neutron beam facility in the country is capable of handling a steel ring 6 feet in diameter, so at this time, plans to analyze mockup weld residual stresses by using neutron diffraction have been shelved.

4.1.4 Stress Measurement Locations and Methods for the Mock-Up

In order to completely characterize the residual stresses associated with the welds in the mock-up, a combination of the techniques described above will be employed. Combining the measurements will mitigate the errors/uncertainties associated with any one method. The container will be cut at Ranor in the center of the middle segment (i.e., at the midpoint between the two circumferential welds) as shown in Figure 3. One section will be sent to the facility performing deep-hole drilling and contour measurements, Veqter Ltd. of Bristol, United Kingdom. During the cutting process, surface-mounted strain gauges will be used to measure relaxation that might occur due to loss of constraint, so that it can be added back into the measured residual stresses later, if necessary. The other half of the mockup will be used for other characterization and testing activities, as described later in this report.

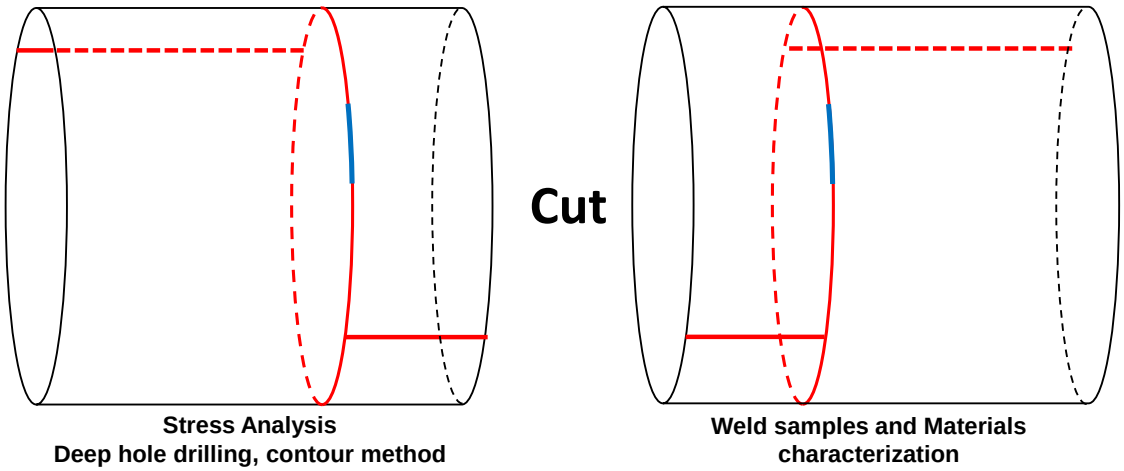

Figure 3: Plan for sectioning the container into two segments, one for weld samples and materials characterization and the other for residual stress measurements using deep-hole drilling and contour method measurements.

Measurements will be made in five different regions, as illustrated schematically in Figure 4. These regions include the circumferential and longitudinal welds, as well as at the end and across the center of the repair regions. Finally, the stress state of the base metal will be measured. The following measurements are planned.

Circumferential weld and Longitudinal weld:

a. Deep hole drilling measurement in center of fusion zone

b. Deep hole drilling measurement in heat affected zone (immediately adjacent to fusion zone)

c. Contour measurement perpendicular to weld centerline

d. (optional) Contour measurement along weld centerline (parallel to centerline)

Center and end of weld repair region:

a. Contour measurement perpendicular to weld centerline

b. (optional) Contour measurement parallel to weld centerline (in center of weld)

c. (optional) Deep hole drilling measurement in center of weld fusion zone (center of repair)

Base metal:

a. Deep hole drilling measurement

When performing the deep hole drilling measurements, the holes will be drilled prior to any sectioning for removing contour measurement coupons. Each time the container is cut, the holes will be re-characterized. Once they are at their final size, the EDM overcore will be performed, and then the holes characterized one final time. As a result, the series of measurements will provide an assessment of the degree of stress relaxation associated with the gradual reduction in size of the workpiece. This information will be of critical importance when determining how the welds will be sectioned for SCC initiation testing as described below.

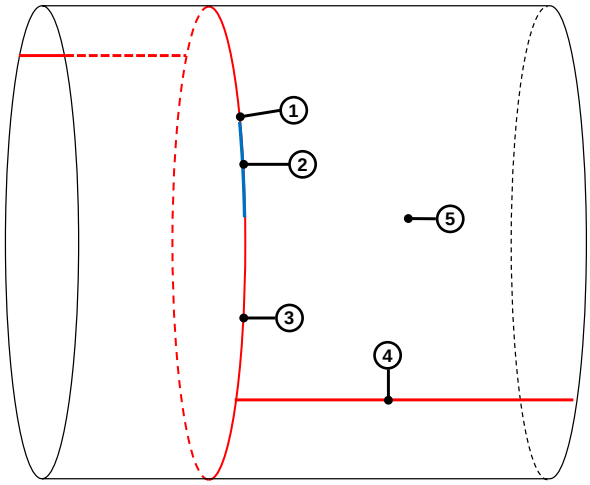

Figure 4: Regions for residual stress measurements. (1) End of repair region, (2) Center of repair region, (3) Circumferential weld, (4) Longitudinal weld, and (5) Base metal

4.2 Weld Metallurgical Condition and Degree of Sensitization

Assessment of the microstructure of the regions at the longitudinal, circumferential, and repair welds will be performed using standard metallurgical techniques. An effort will be made to perform these analyses in the same basic regions as the residual stress measurements such that the two can be correlated.

The thermal cycling associated with the welding process, in addition to altering the overall microstructure of the near-weld material, can result in the precipitation of chromium-rich carbides and the concomitant formation of chromium depleted regions along the grain boundaries. This effect, known as sensitization, will be particularly pronounced in the weld heat affected zone (i.e., material in a region near the weld fusion zone that is heated to peak temperatures up to the effective solidus). The extent to which

sensitization has taken place will be documented as a function of position from the edge of the weld fusion zone. This will be done both for the near surface regions, as well as through the thickness of the container wall. A volumetric assessment of the degree of sensitization will illustrate the extent of the region and illustrate the presence/absence of an active path for crack propagation through the material.

Samples taken from the container will be prepared metallographically and evaluated electrochemically for the degree of sensitization. Evaluation will be done through either the single loop electrochemical reactivation (EPR) test or double-loop EPR test. For the single loop test, as defined in American Society for Testing and Materials (ASTM) specification G108 "*Standard Test Method for Electrochemical Reactivation (EPR) for Detecting Sensitization of AISI Type 304 and 304L Stainless Steels*" (ASTM 2010), the surface to be analyzed is polarized anodically such that the surface is activated. This results in enhanced dissolution of the chromium depleted grain boundaries, while the remainder of the grain is rendered passive. The net charge associated with dissolution of the chromium depleted regions along the grain boundaries is determined based upon the total current passed during the aforementioned polarization. This technique requires characterizing the microstructure of the material (specifically, the grain size), such that the overall charge per unit area of grain boundary can be calculated, the magnitude of which defines the extent of sensitization. The second technique is a modification of the first, and is more suitable for instances where the surface finish of the material being evaluated is less well defined, or measurement of the grain size within the material is difficult. This technique, described in Scully (1995) is known as the double-loop EPR technique. In this method, the sample is essentially subjected to the same polarization as the single loop EPR, but it is applied twice. The ratio of the peak currents extracted from the first and second polarization is then recorded. The magnitude of this ratio is directly related to the degree of sensitization of the material. For an un-sensitized microstructure, the first polarization passivates the sample, such that the peak current from the second polarization is considerably lower than the first. However, in the case of a sensitized microstructure, the chromium depleted zones are not passivated by the first polarization, and the peak current for the second polarization will be large, approaching the value of the first polarization. The magnitude of the ratio is used to assess the degree of sensitization, with the value approaching 1 for heavily sensitized materials.

In the event that the electrochemical techniques are insufficient to define the degree of sensitization of the container wall material, alternate methods will be pursued, such as those defined in ASTM A262 "*Standard Practices for Detecting Susceptibility to Intergranular Attack in Austenitic Stainless Steels*" (ASTM 2014). This specification provides a series of immersion tests designed to activate grain boundaries such that the extent of attack can be assessed either via metallography or weight change measurement.

Positional mapping of the degree of sensitization will be accomplished by selectively mapping regions of the surface using plating tape or a similar material. The exposed region will be selected such that a sufficient number of grains are evaluated in each test. Replicate measurements will be accomplished by grinding the surface upon the completion of the each successive set of experiments, such that the region immediately below the first set of measurements can be performed. This procedure will be repeated for each of the regions where the stress distribution is assessed (i.e., the circumferential, longitudinal, and repair welds).

4.3 Stress Corrosion Cracking Susceptibility

Establishing the susceptibility to SCC will require both the resistance to crack nucleation as well as the magnitude of crack propagation to be assessed as a function of the environmental conditions to which the container is subjected while exposed to stresses as defined by the full scale mock-up. A wide variety of experiments are planned,

1. The information learned from the residual stress measurements, combined with the electrochemically determined degree of sensitization will enable the fabrication of material simulating the weld heat affected zone. The samples will be subjected to the same

thermomechanical processing to which the HAZ has been subjected using a Gleeble, a simulator capable of replicating the thermal and mechanical history of the HAZ . These samples will then be used in simple U-bend experiments, where marine aerosols are deposited on the surface of the bent portion of the sample (replicating the surface deposits observed via in-service inspections, as well as predicted worst-case deposits), then subjected to combinations of humidity and temperature typical of coastal ISFSI sites. These experiments will be used to evaluate SCC initiation under relevant conditions and with relevant materials and stresses.

2. Crack propagation studies will be conducted using compact tension specimens where the microstructure has been modified so as to accurately simulate the condition in the heat affected zone of actual storage containers, and tensile stresses will cover the range of residual stresses measured in the mockup welds. The surface deposits and exposure conditions will be similar to those explored for U-bend specimens.

Specimens taken from the large scale mockup, sized so as to maintain a residual stress distribution similar to that for the as-received condition, will be used for crack initiation and propagation studies. A combination of worst case and field representative deposits will be placed on the surface of the samples, after which they will be exposed to relevant temperature and humidity conditions. It should be noted that mockup samples will be relatively large and limited in number, so the aforementioned tests will be used to define the conditions used to evaluate specimens taken from the mock-up.

5. STATUS OF THE CHARACTERIZATION WORK

5.1 Sectioning of the Mockup

As described in the previous sections, the mockup cylinder is intended to be used in several different ways. One main goal is to measure weld residual stresses, and this must be done on a large cylindrical section of the mockup, in order to capture the effects of the cylindrical constraint on the stresses. Other parts of the mockup will be used for material characterization studies, and for testing techniques for non-destructive evaluation (NDE) of canister surfaces for SCC cracks. The mock-up has been subdivided into three sections, as indicated in Figure 5. The largest of the three sections will be used to assess the residual stress state of the weldments and base metal using techniques described in Section 4.1 and detailed below for this specific application. The second section will cut into pieces to provide samples of both the longitudinal and circumferential welds to the UFD program for the assessment of SCC susceptibility. The first section will also be cut into samples upon completion of residual stress analyses. The final section was taken from the base of the container and was provided to EPRI as a mock-up for testing NDE techniques. The location of each section on the actual mockup is shown in Figure 6a.

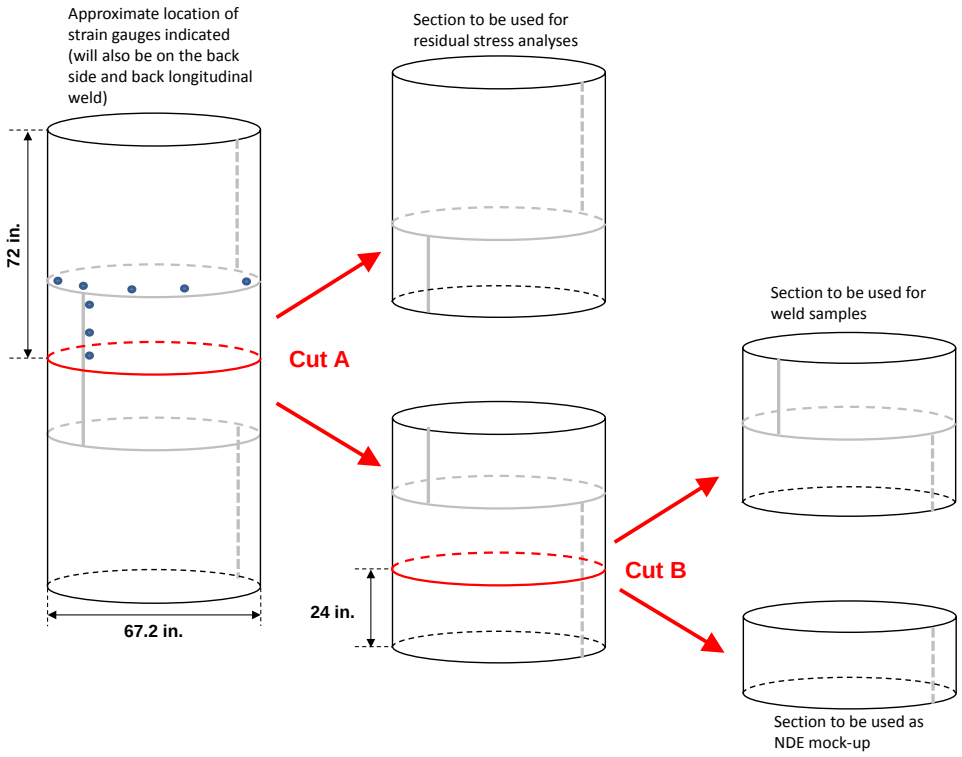

Figure 5: Cut plan used to subdivide the container into sections for residual stress analysis and test coupons.

Figure 6: Mock-up container prior to being sectioned. (a) Location of three sections into which the container was cut – one for residual stress analysis (A) and two for specimens (B and C). A temporary spider (b) was placed just below the cut made between sections A and B in order to minimize distortion as the cut was made.

Cutting of each section was performed using a 1" roughing end mill. Each cut was made as a series of four smaller cuts, leaving an approximately 0.25" ligament between each cut. These ligaments served to stabilize the container while cutting. In addition, to minimize distortion within the container, the container was reinforced internally using a spider as shown in Figure 6b. The spider was positioned immediately below the cut between the upper section (to be used for residual stress analysis) and the lower section (to be used for specimens). The spider was temporary and removed upon completion of the cut, leaving no visible deformation upon removal. In addition to the spider, four temporary blocks were welded to the end of the container to allow it to be secured to the rotary table used during the cutting operation. These blocks were 1" x 2" x 3" in size and were removed upon completion of the cut. All four are located on the lower section designated "C" and were far from any locations used for surface strain measurement, as illustrated in Figure 7.

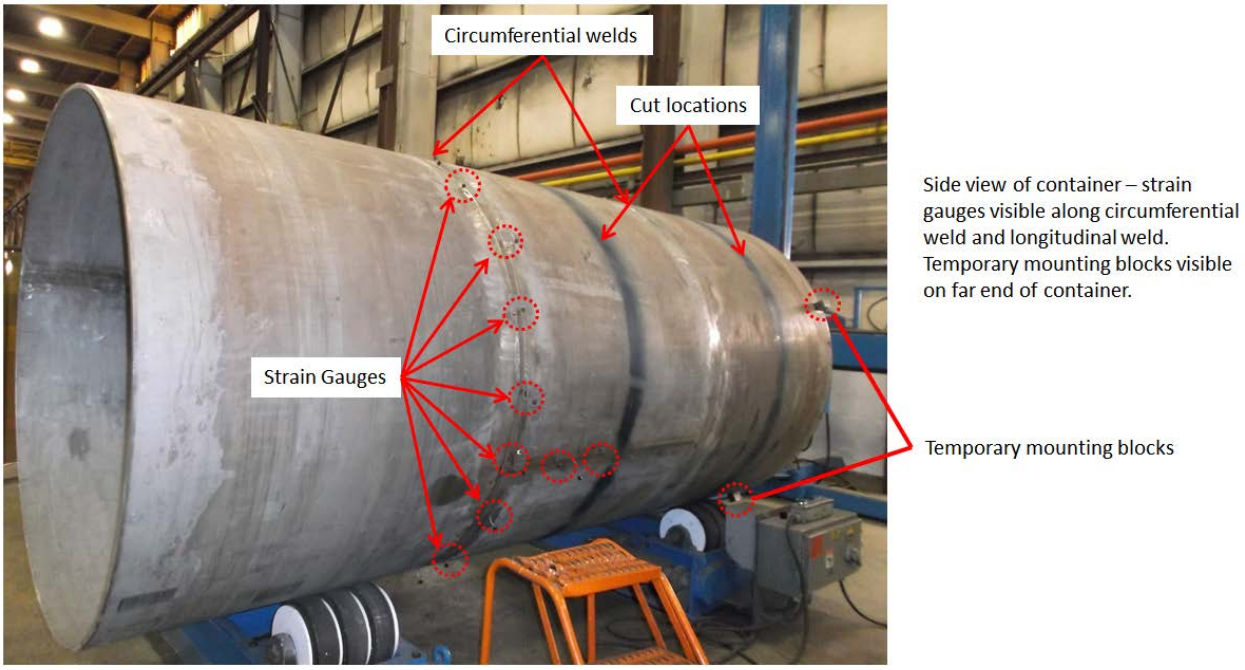

Figure 7: Location of surface strain gauges positioned along the longitudinal and circumferential welds. Also shown is the position of the temporary mounting blocks welded to the base of the container to facilitate positioning while the cuts were being made.

There are two primary sources of residual stress within the container, the origin of which is best illustrated by a discussion of how the cylinder was formed. The raw material used to form each of the three segments of the cylinder was received in the form of annealed plate. These plates were then deformed into a cylinder – a process which is accomplished by gradually bending the plate, introducing significant plastic deformation of the material, and a complex stress state through the thickness of the wall. Once formed into cylinders, each plate was then welded. When the weld is made, the liquid metal in the weld pool solidifies, and in the process, contracts. Since this contracting material is effectively held in place (i.e., constrained) by the overall structure of the cylinder, the degree to which the solidifying metal can contract is limited, and as a result the solidified weld has a considerable tensile residual stress. Similarly, the material away from the weld root is also impacted by the attempted contraction of the weld, and as a result it is under a considerable compressive residual stress. It is the combination of these two stresses (formation and welding) that form the driving force for any potential stress corrosion cracking.

When the container is subdivided by cutting, the constraint on which each portion of the container by the overall structure is changed, allowing for macroscopic deformation as the stresses relax. In order for the stresses within the as-manufactured container to be measured accurately, any such relaxation due to the cutting operation must be measured and accounted for.

To measure any relaxation that occurred during cutting, surface-mount strain gauges were positioned along the longitudinal and circumferential welds at 10 inch intervals. While relaxation might be greater closer to the cut, the weld regions are the critical areas, as they are where WRS will be later be measured. A total of 28 strain gauges were utilized. In Figure 7, the position of some of these gauges is illustrated. The gauges themselves consisted of two designs procured from Vishay Precision Group, and are illustrated in Figure 8. Each strain gauge is a tee rosette consisting of two separate sensors, one of which was aligned parallel to the length of the container (denoted axial strain) and the second aligned parallel to the circumference of the cylinder (denoted hoop strain). Prior to affixing each sensor, a location was identified where there were no macroscopic scrapes/scratches present as in order to function properly, the sensor must be in intimate contact with the underlying substrate. The container surface was then cleaned using isopropyl alcohol, and an anchor pattern was applied using 240 grit SiC abrasive paper. The anchor pattern itself consisted of a cross-hatched pattern formed by using the abrasive in the lateral direction, followed by the axial direction. Once the anchor pattern was placed, the surface was cleaned again with isopropyl alcohol, after which it was etched using Vishay M-Prep Conditioner-A (a mild phosphoric acid solution). Once etched, the surface was neutralized using Vishay M-Prep Neutralizer 5A (an ammonia based solution). Next, the strain gauge was placed on a segment of Vishay PCT-2M gauge installation tape. The mounting surface of the gauge was then coated with M-Bond 200 adhesion promoter, followed by the M-Bond 200 adhesive (a cyanoacrylate adhesive) and the strain gauge was adhered to the container surface. Once the adhesive cured, leads were soldered to each of the four terminals shown in the figure. The completed gauge was then covered with a urethane coating to protect it from surface damage, and the leads secured to the surface of the container using tape.

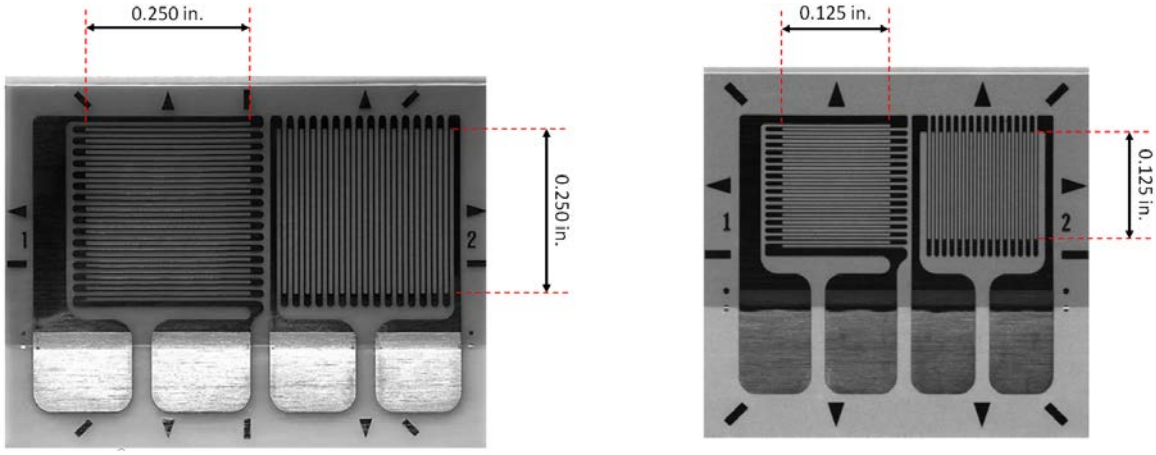

Figure 8: Surface strain gauges used to monitor the strains associated with cutting the mock-up container. Most of the sensors were part number CEA-00-250UT-350 (a) along with two smaller CEA-06-125UT-350 (b) strain gauges. Functionally, the two are identical.

Each strain gauge functions as a resistor, with a resistance of 350 ohms. As the surface moves due to stress relaxation, the dimensions of the strain gauge and its resistance also change. Gauges were positioned along both the circumferential and longitudinal welds as illustrated in Figure 9. In locations

where the circumferential weld intersected with a longitudinal weld, three gauges were positioned as illustrated in Figure 9b. Once positioning of the sensors was complete, initial measurements were made to calibrate each of the sensors (Figure 10a). After the initial measurements were made, the container was cut. As one of the sensors was close to the cut region, care was taken to protect that sensor and to prevent coolant splash or tooling damage. Once cutting was complete (Figure 10b), the sensors were monitored again, and the resulting difference in resistance transformed to an equivalent surface strain. In addition to the half of the cylinder reserved for strain analysis, the other half was sectioned into two pieces, as illustrated in Figure 11, for other uses.

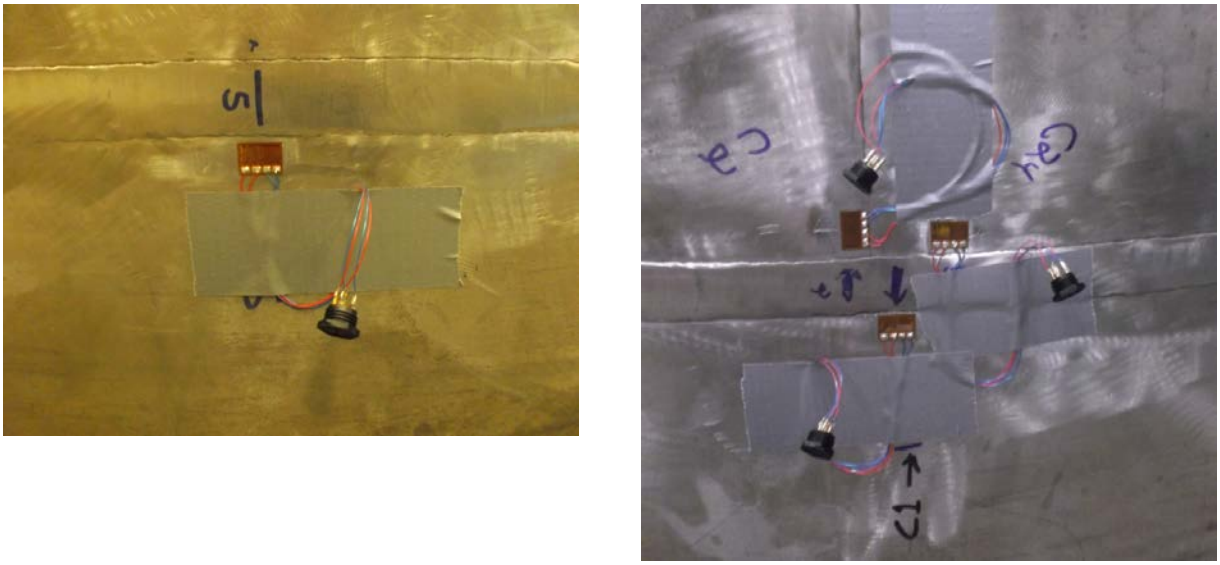

Figure 9: Surface strain gauges were positioned along the longitudinal and circumferential welds. Gauges were placed as close to the weld fusion zone as possible (a). In addition, a series of three sensors were positioned in each location where a circumferential weld intersected with a longitudinal weld (b).

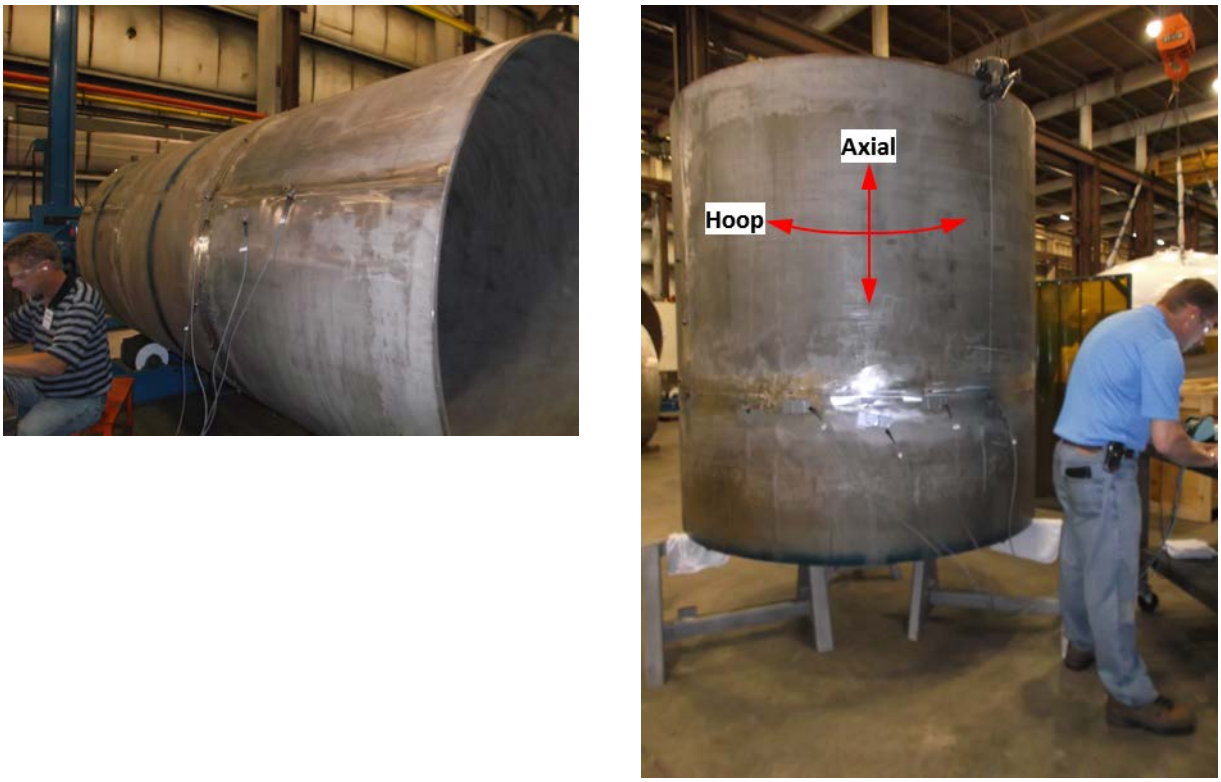

Figure 10: Measurement of strain gauges before (a) and after (b) cutting the container. The data acquisition system enabled four sensors to be monitored at a time, so that they were evaluated in groups. Sensors were measured using the same channel for the initial and final measurements.

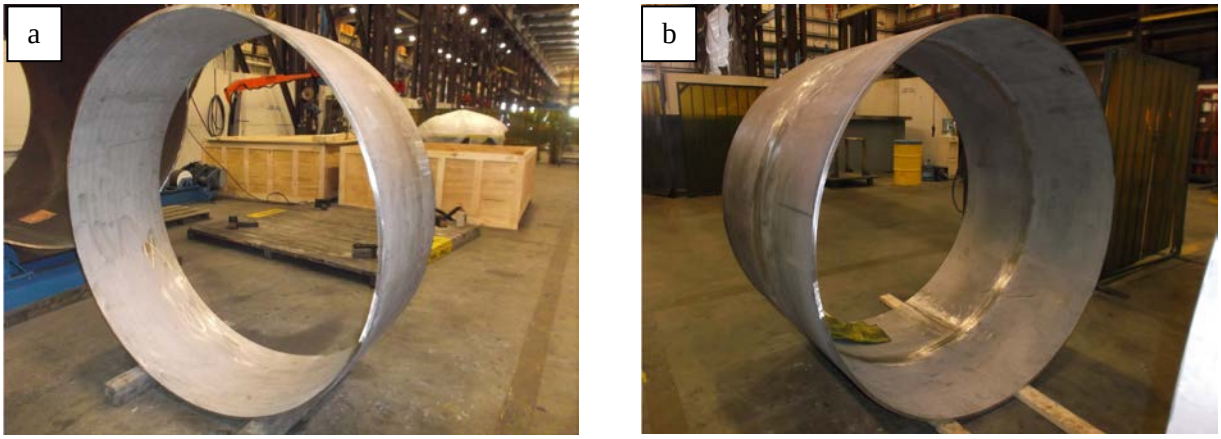

Figure 11: Container was cut into three segments, a 6-foot section used for residual stress analysis (Figure 10); a 2-foot segment for use by EPRI as a small-scale mockup for NDE sensor testing (a); and 4-foot segment for cutting into weld samples for SCC and microstructural characterization (b).

The surface strains measured for the circumferential weld are presented in Figure 12. In terms of their orientation, strains that are parallel with the long dimension of the container are termed “axial strains” and strains that are around the circumference/round dimension of the container are termed “hoop strains”. There are two longitudinal welds that intersect with the circumferential weld. The weld which was cut is termed the lower weld, and the uncut weld is termed the upper weld.

The strains along the circumferential weld (Figure 12) were small (microstrain) and primarily tensile in nature, and represent the resolution of the technique as implemented here. At the location where the lower weld (the weld which was cut through) intersected the circumferential weld, the strains were larger, and compressive in the hoop direction (i.e., parallel to the circumference of the container), but remained tensile in the axial direction.

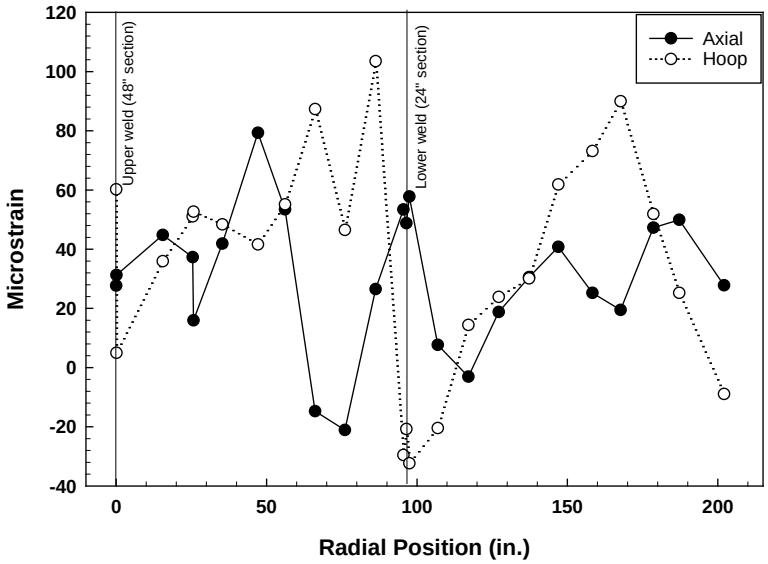

Figure 12: Surface strain measurements along the circumferential weld. Note that the sensors are located approximately 10 inches apart (with exceptions as noted above) and that the overall circumference was 211 inches (i.e., a point at 0” is in the same location as a point at 211”).

As discussed previously, sensors were placed alternatively on the upper and lower shell. To evaluate if there was a difference between the strains experienced by the upper and lower shell, the axial (Figure 13a) and longitudinal (Figure 13b) strains were plotted as a function of which shell the respective strain gauge was located. As can be seen in the figure, there is no difference between the two shells (on either side of the circumferential weld).

Measurements were also made along the upper and lower longitudinal welds. The data for the upper weld is illustrated in Figure 14a. As can be seen in the figure, the strains were comparable in magnitude to those around the circumferential welds (i.e., microstrain). Strains were consistently tensile in the Axial direction and compressive in the Hoop direction. The measurements made at the lower longitudinal weld (Figure 14b) illustrate that significant deformation of the end of the container resulted from the cut. The In the longitudinal direction, the strain was tensile, while in the axial direction it was primarily compressive. This indicates that cutting the container in half resulted in a loss of constraint in the regions near the cut. As a result, the stresses from the circumferential weld (tensile hoop stress) resulted in the end of the container becoming smaller in diameter and lengthening slightly. Visually, the container could be considered to be necking down as the location of the cut is approached. Moving further from the cut, the constraint provided by the remaining structure prevented significant surface strain.

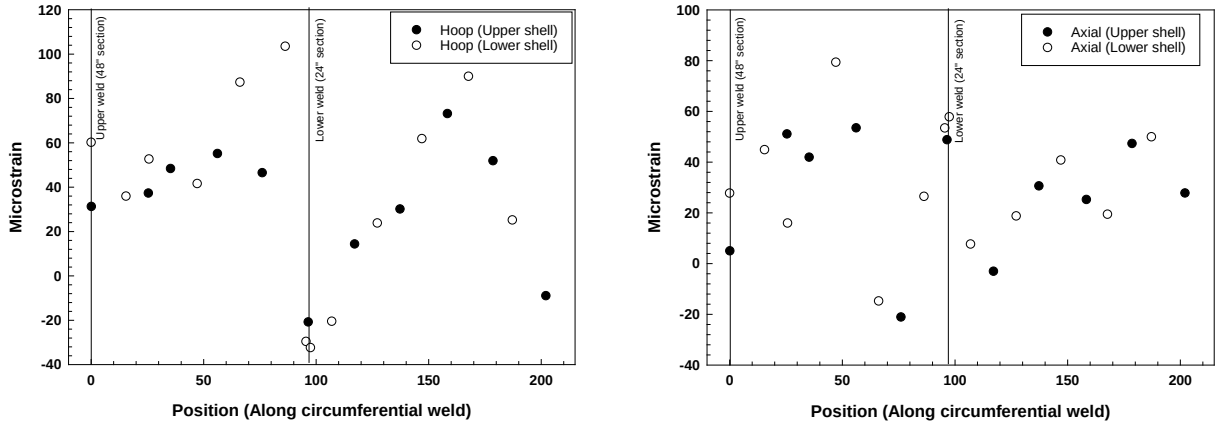

Figure 13: Hoop (a) and Axial (b) strains as a function of position around the circumferential weld, further noted as to which shell the strain gauge was located on.

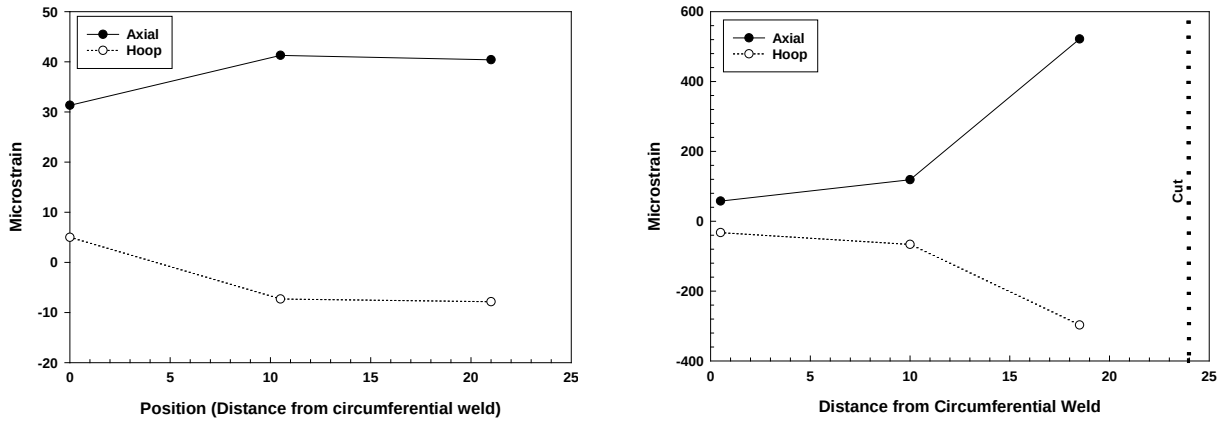

Figure 14: Axial and Hoop strains were measured along the upper (a) and lower (b) longitudinal welds. The lower weld is the one which was cut.

5.2 Residual Stress Measurements

As discussed above, the residual stresses associated with weldments are the likely mechanical driving force that would support SCC crack propagation through the container wall. To date, iCHD and DHD has been performed on the bulk material far from a weldment (location 5 in Figure 4). The concern has been raised that crack initiation may take place on surfaces away from the weld, in which case the residual stresses from the forming process for the container would be the likely driving force.

As the deep hole drilling technique is inaccurate near the outer metal surface, center hole drilling was used to measure the stresses in the first 0.5mm of material. In this technique, a strain rosette similar to that pictured in Figure 15 is placed on the surface to be analyzed, and then a hole is precisely drilled through the center of the pattern. The positioning of the drilling tool is illustrated in Figure 16a, and the resulting hole, surrounded by the strain gauge rosette, is shown in Figure 16b. As the hole is drilled, the

stress relaxes in the region near the hole, the resulting strains from which are monitored by the strain gauges described above. These strains are then converted to the effective stresses near the surface.

Figure 15: Strain gauge rosette used to perform iCHD measurements. As the hole is drilled at the circular indication in the center of the pattern strains are measured in three directions, 120 degrees apart.

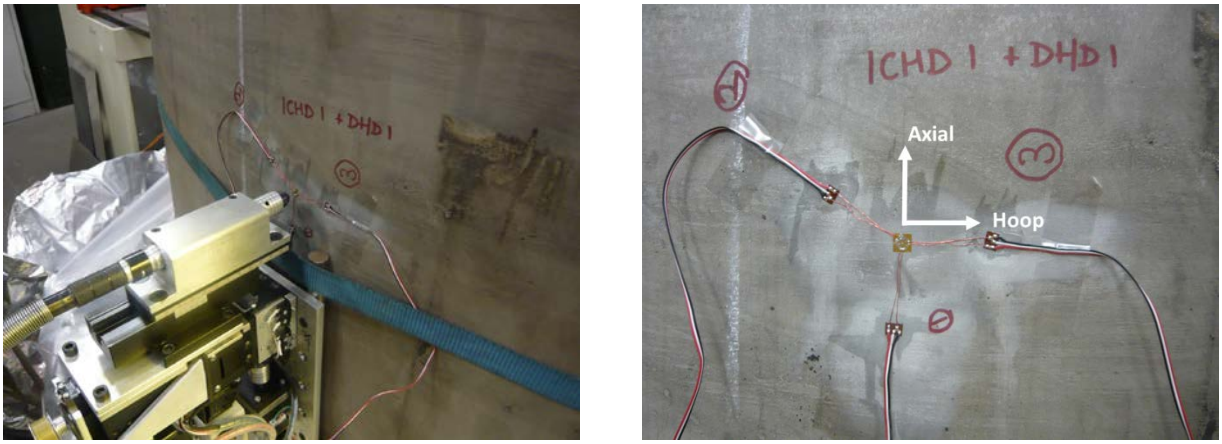

Figure 16: Mechanism used to perform iCHD measurements in the base metal (far from the longitudinal and circumferential welds). Drilling equipment is shown in (a) and the orientation of the strain gauge relative to the axial and hoop directions is illustrated in (b).

The resulting iCHD stress distribution is shown in Figure 17. As a point of reference, the yield strength of annealed 304L SS is on the order of 170-200 MPa. Very near the surface, the residual stresses were tensile in nature. However, as you move into the material, the axial strain remains small and tensile, but the hoop stress becomes compressive in nature. While the data shows a relatively high shear stress in the near surface region, caution must be used when interpreting this result. In order to perform the iCHD measurements in the same location as a subsequent DHD measurement, a very small strain rosette must be used as the diameter of the hole drilled for the iCHD measurement must be smaller than that of the DHD reference hole to prevent the first measurement influencing the second. As a result, the smaller strain gauge samples a smaller effective volume of material, leading to an increased signal–to-noise ratio and a corresponding increased uncertainty. Also, due to the small size of the strain gauges, any misalignment or eccentricity of the drilled hole, i.e. experimental error, will be more apparent in the results. The error bars only reflect the magnitude of the uncertainties that can be directly measured, such

as curving fitting error and Young's Modulus uncertainty, and not measurement uncertainty as discussed above. As such, the data in the figure is best interpreted in terms of the average magnitude and trends, which indicates low residual stresses in the first 0.5mm from the OD of the container.

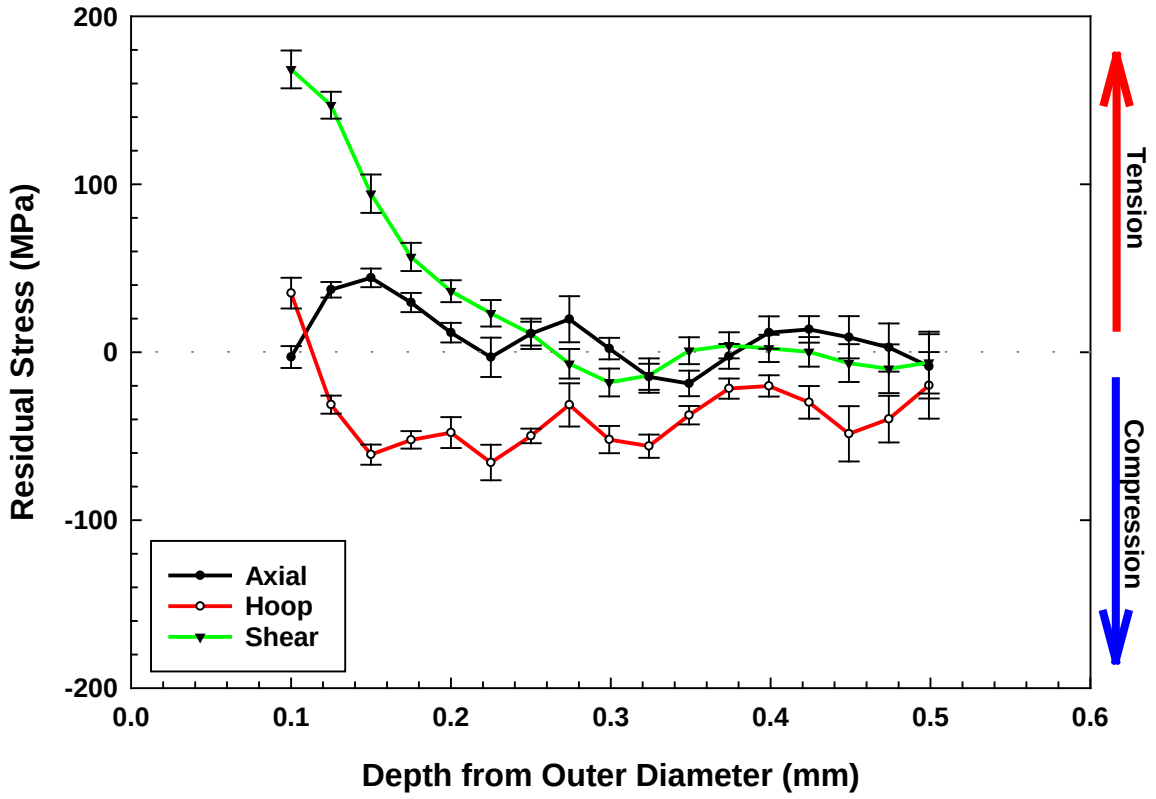

Figure 17: iCHD data for region located for a base-metal region located far from any longitudinal or circumferential weldments.

For the stress distribution through the thickness of the container wall, deep hole drilling (DHD) was performed. In Figure 18, the equipment used to align and stabilize the measurement equipment is shown, along with the directions of each stress that was measured. The region measured is far from the welds, and the anticipated stresses are small relative to the yield strength of the material, so incremental DHD was not necessary.

Figure 18: Positioning equipment used to perform DHD measurements of a base metal region (far from any weldments). The orientation of the axial and hoop stresses is indicated on the figure. In the center of the fixture, the hole and EDM overcore can be seen.

The stress distribution through the container wall is shown in Figure 19. Note that data from the near-surface region are not presented in this figure – data for that region were obtained via iCHD and are reported in Figure 17 above. The stress state in the container wall is predominantly tensile in nature in both the axial and hoop directions. Moving further into the wall, the hoop stress becomes increasingly tensile, then both the hoop and axial stresses decrease to approximately zero in the center of the wall. Both the hoop and axial stresses then become large and compressive in nature until reaching the inner surface where they again become tensile in nature. The origin of these stresses is illustrated schematically in Figure 20 which shows a flat plate being bent. As the plate is bent, the outer diameter is placed in tension, while the inner diameter is placed in compression. In an ideal case, the stress distribution would show a uniform transition from tension to compression through the thickness of the wall. However, the formation process is not ideal, and the transformation of the plate into a cylinder is done in a stepwise fashion. Through this process, only a small portion of the plate is bent in each step, and as a result the stress state is more complex.

The stress profile through the canister shell illustrates why through-thickness cracking is not anticipated at regions away from the weld. While crack initiation can take place at the surface, as the crack grows into the wall, the tensile stresses driving crack propagation will decrease, eventually becoming compressive in nature and arresting crack propagation.

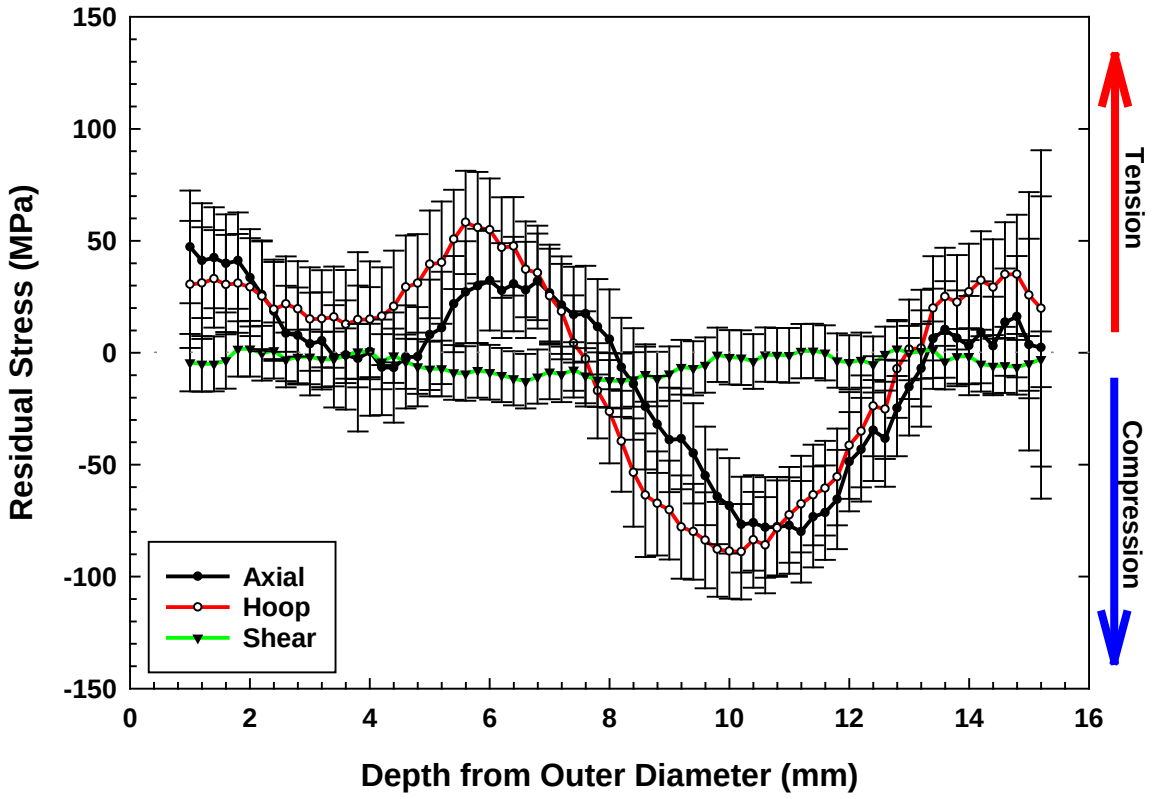

Figure 19: DHD data as a function of distance from the outer diameter of the container for a region located far from any weldments. Note that stresses are tensile near the surfaces, then become compressive in the center of the wall due to the deformation process used to form the original plate material into a cylinder.

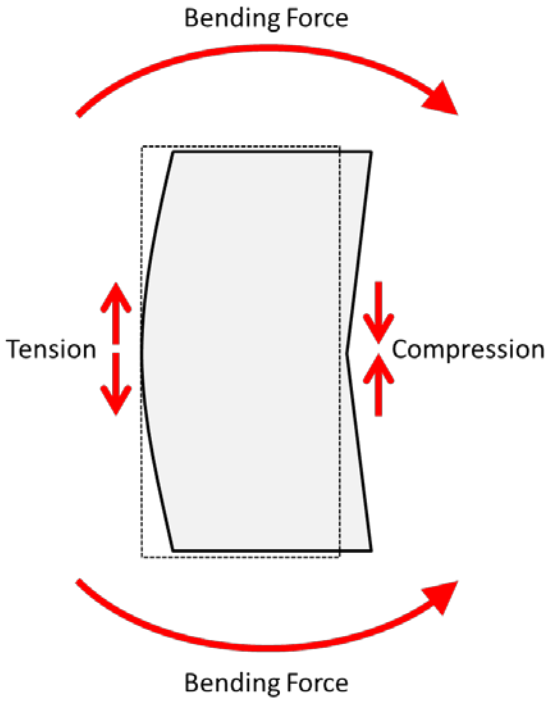

Figure 20: Schematic representation of the forces resulting from bending the plate material used to construct the mockup into a cylinder. Note that this indicates the general forces, and does not capture the near surface deformation resulting from the formation process (which is done in steps, and as such can result in tensile surface stresses, even at the inner diameter of the wall).

5.3 Schedule for Additional Measurements

To date, only a single location, representing base metal far from any weldments, has been analyzed for residual stresses. A schedule has tentatively been developed for the additional work described in Section 4.1. Stresses associated with one circumferential weld will be measured by iCHD and iDHD prior to the end of August, 2015. Other weld locations will be characterized using these methods in September and October. In November, prior to cutting the mockup into pieces to apply the contour method, work will be paused, and the existing data sets will be evaluated to ensure that no further analysis of the intact mockup is required. Then, from December to February, 2015, the mockup will be sectioned, while periodically measuring the amount of stress release by monitoring at least one of the existing DHD holes, and then, contour analyses will be carried out on regions close to, and structurally identical to, the areas where DHD testing was done (DHD affects the residual stresses in areas within a few centimeters of the hole). The current schedule indicates that weld residual stress analyses should be entirely completed by March 2015.

Once the stress analyses are completed, the information gathered will be used to determine the appropriate size for weld samples, in order to retain as much of the weld residual stresses as possible. Then, the mockup section at Sandia, and the remaining material from the half used for stress analyses will be cut into pieces to provide weld samples for material characterization and corrosion testing. The cutting should be complete by summer, 2016.

6. WELD SAMPLE DISSEMINATION TO INTERESTED PARTIES

The mockup weld samples, in addition to being critical for the UFD program, are also of great interest to outside parties such as EPRI and academic groups working on storage-related NEUP programs. Meetings will be held with each of the interested parties to assess their needs. Utilizing the information from each party, a larger prioritized list of coupons will be assembled. The needs of the UFD program will be given first priority, followed by the DOE funded NEUP groups and EPRI.

7. SUMMARY

Uncertainties exist both in terms of the environmental conditions that prevail on the surface of SNF interim storage canisters and the electrochemical properties of the storage containers themselves. To address those uncertainties, the DOE has procured a full-diameter cylindrical mockup of a storage canister, produced using the same manufacturing procedures as fielded canisters. This document describes the design and procurement of the mockup and the planned characterization work. It also provides the status of the project, describing the cutting of the mockup into sections for different analyses, and presenting initial results from the stress characterization effort.

In order for SCC to be a viable degradation mode, three criteria must be met – there must be a sufficiently large stress in the material to support crack growth, the material itself must be susceptible to stress corrosion cracking, and the environment must be sufficiently aggressive to support crack initiation and propagation. The work described in this document is aimed at evaluating the first two of these criteria for in-service containers by characterizing the material properties of the base metal and weld zones on the canister mockup. Assessment of residual stresses associated with forming and welding was performed using a combination of three techniques. These include deep-hole drilling, the contour method, and x-ray diffraction. The deep-hole drilling technique allows measurement of residual stresses along a one-dimensional hole drilled through the wall of the cylinder; it allows measurement of stresses within the intact cylinder and hence, captures the effects of the cylindrical constraint on the stresses. The contour method provides a two-dimensional map of stresses along a cross section through a region of interest; however, the mockup must be cut into pieces to measure the face of the cross section, and stresses due to the constraint of the intact cylinder are lost. X-ray diffraction allows assessment of very shallow near-surface stresses, and potentially phase changes (e.g., formation of deformation-induced martensite), associated with shaping and grinding the mockup. It is also used to map stress components that are in-plane with the cross sectional surface, when using the contour method.

Characterization of residual stresses in the mockup has begun. After fabrication, the mockup was cut into three sections. The largest section was reserved for residual stress measurements; the other two pieces will be used for material characterization studies and testing of SCC evaluation methods. During the cutting process, strain gauges were used to monitor stress relaxation at locations where weld residual stresses will ultimately be measured, so that it can be added back in, if necessary, to obtain the as-manufactured residual stresses. However, measured strains were very small, and can be ignored; cutting the cylinder in half had little effect on residual stresses. One set of stress measurements has been collected to date, at a base metal location far from any weld. The iCHD technique was used to measure very shallow stresses (<0.5 mm), while the iDHD technique was used to measure the through-thickness stress profile. Results indicate that in this non-welded region, residual stresses are dominated by those introduced during the forming of the plate to make a cylinder. The curling process extended the outer surface of the shell while shortening the inner surface, and the residual stresses reflect this. Except for near-surface regions, the other half of the shell wall is under tension, while the inner half of the shell is under compression. These data will provide a baseline for the residual stresses near the weld zones, to be measured in coming months.

Evaluation of the electrochemical properties of the welded regions of the container will first involve an assessment of the microstructure of the regions at the longitudinal, circumferential, and repair welds via standard metallurgical techniques. The thermal cycling associated with the welding process will, in addition to altering the overall microstructure of the near-weld material, result in the precipitation of chromium carbides and the formation of chromium-depleted regions along the grain boundaries. This effect, known as sensitization, will be particularly pronounced in the weld heat affected zone (i.e., the region near the weld fusion zone that has been impacted by the heat input from the welding process). The extent to which sensitization has taken place will be documented as a function of position from the edge of the weld fusion zone. This will be done both for the near-surface regions and through the thickness of the container wall. A volumetric assessment of the degree of sensitization will illustrate the extent of the affected region and illustrate the presence/absence of an active path for crack propagation through the material.

Establishing the storage canister susceptibility to SCC will require both the crack nucleation and crack propagation processes be assessed using samples with relevant crystallographic textures and electrochemical properties, under typical environmental conditions under stress conditions as defined by analyses of the full scale mock-up. A variety of experiments are planned to evaluate both aspects of the cracking process, as well as to define methods to produce relevant weld analog materials.

Upon completion of the residual stress measurements, the mock-up will be sectioned to provide samples for stress corrosion cracking initiation tests. These coupons are critical for the UFD program, but also are of great interest to outside parties such as EPRI and the academic groups working on canister SCC as part of the DOE NEUP programs. Samples will be disseminated to interested parties on an as-needed basis, with the UFD program getting first priority, followed by the DOE-funded NEUP groups and EPRI.

8. REFERENCES

ASTM. (2010). *Method G108-94 (2010): Standard Test Method for Electrochemical Reactivation (EPR) for Detecting Sensitization of AISI Type 304 and 304L Stainless Steels*. West Conshohocken, PA. ASTM International.

ASTM. (2014). *Method A262-14: Standard Practices for Detecting Susceptibility to Intergranular Attack in Austenitic Stainless Steels*. West Conshohocken, PA. ASTM International.

Benson, M., Rudland, D. J. and Csontos, A. (2014). *Weld Residual Stress Finite Element Analysis Validation: Part 1, Data Development Effort*, NUREG-2162. U.S. NRC.

Bouchard, P., George, D., Santisteban, J., Bruno, G., Dutta, M., Edwards, L., Kingston, E. and Smith, D. (2005). Measurement of the residual stresses in a stainless steel pipe girth weld containing long and short repairs. *International Journal of Pressure Vessels and Piping* **82**, 299-310.

Bryan, C. R. and Enos, D. (2014). *Analysis of Dust Samples Collected from Spent Nuclear Fuel Interim Storage Containers at Hope Creek, Delaware, and Diablo Canyon, California*, SAND2014-16383. Albuquerque, NM. Sandia National Laboratories.

Bryan, C. R. and Enos, D. G. (2015). *Analysis of Dust Samples Collected from an Unused Spent Nuclear Fuel Interim Storage Container at Hope Creek, Delaware*, SAND2015-1746. Albuquerque, NM. Sandia National Laboratories.

Cook, A., Lyon, S., Stevens, N., Gunther, M., McFiggans, G., Newman, R. and Engelberg, D. (2014). Assesing the Risk of Under-Deposit Chloride-Induced Stress Corrosion Cracking in Austenitic Stainless Steel Nuclear Waste Containers. *Corrosion Engineering, Science and Technology* **49**, 529-534.

Cook, A., Stevens, N., Duff, J., Mishelia, A., Leung, T. S., Lyon, S., Marrow, J., Ganther, W. and Cole, I. (2011). Atmospheric-induced stress corrosion cracking of austenitic stainless steels under limited chloride supply. *Proc. 18th Int. Corros. Cong., Perth, Australia*.

Dong, P., Hong, J. and Bouchard, P. (2005). Analysis of residual stresses at weld repairs. *International Journal of Pressure Vessels and Piping* **82**, 258-269.

Dong, P., Zhang, J. and Bouchard, P. (2002). Effects of repair weld length on residual stress distribution. *Journal of pressure vessel technology* **124**, 74-80.

Elcoate, C., Dennis, R., Bouchard, P. and Smith, M. (2005). Three dimensional multi-pass repair weld simulations. *International Journal of Pressure Vessels and Piping* **82**, 244-257.

Enos, D. and Bryan, C. (2014). *Technical Work Plan: Characterization of Weld Regions on a Full-Scale Cylindrical Mockup of an Interim Storage Container*, FCRD-UFD-2014-000710. Albuquerque, NM. U.S. Department of Energy.

Enos, D. G., Bryan, C. R. and Norman, K. M. (2013). *Data Report on Corrosion Testing of Stainless Steel SNF Storage Canisters*, FCRD-UFD-2013-000324. U.S. Department of Energy, Office of Used Nuclear Fuel Disposition.

EPRI. (2011). *Extended Storage Collaboration Program (ESCP) Progress Report and Review of Gap Analyses*. Palo Alto, CA.

EPRI. (2014). *Calvert Cliffs Stainless Steel Dry Storage Canister Inspection*. Palo Alto, CA.

García, C., Martín, F., De Tiedra, P., Heredero, J. and Aparicio, M. (2001). Effects of prior cold work and sensitization heat treatment on chloride stress corrosion cracking in type 304 stainless steels. *Corrosion Science* **43**, 1519-1539.

Gellrich, G. H. (2013). *Response to Request for Additional Information, Re: Calvert Cliffs Independent Spent Fuel Storage Installation License Renewal Application (TAC No. L24475) dated April 24, 2013*, NRC Adams accession numbers ML13119A242, ML13119A243, and ML13119A244.

George, D. and Smith, D. (2005). Through thickness measurement of residual stresses in a stainless steel cylinder containing shallow and deep weld repairs. *International Journal of Pressure Vessels and Piping* **82**, 279-287.

Ghosh, S. and Kain, V. (2010a). Effect of surface machining and cold working on the ambient temperature chloride stress corrosion cracking susceptibility of AISI 304L stainless steel. *Materials Science and Engineering: A* **527**, 679-683.

Ghosh, S. and Kain, V. (2010b). Microstructural changes in AISI 304L stainless steel due to surface machining: Effect on its susceptibility to chloride stress corrosion cracking. *Journal of Nuclear Materials* **403**, 62-67.

Ghosh, S., Rana, V. P. S., Kain, V., Mittal, V. and Baveja, S. (2011). Role of residual stresses induced by industrial fabrication on stress corrosion cracking susceptibility of austenitic stainless steel. *Materials & Design* **32**, 3823-3831.

Hanson, B., Alsaed, H., Stockman, C., Enos, D., Meyer, R. and Sorenson, K. (2012). *Gap analysis to support extended storage of used nuclear fuel*, FCRD-USED-2011-000136. U.S. Department of Energy.

Hayashibara, H., Mayuzumi, M. and Mizutani, Y. (2008). Effects of temperature and humidity on atmospheric stress corrosion cracking of 304 stainless steel. *CORROSION 2008*.

Hossain, M., Goudar, D., Truman, C. E. and Smith, D. J. (2011). Simulation and measurement of residual stresses in a type 316h stainless steel offset repair in a pipe girth weld. *Materials Science Forum*: Trans Tech Publ, 492-497.

Hossain, S., Truman, C., Smith, D. and Bouchard, P. (2006). Measurement of residual stresses in a type 316H stainless steel offset repair in a pipe girth weld. *Journal of pressure vessel technology* **128**, 420-426.

Kain, R. M. (1990). Marine atmosphere corrosion cracking of austenic stainless steels. *Materials Performance* **29**, 60-62.

Khatak, H., Gnanamoorthy, J. and Rodriguez, P. (1996). Studies on the influence of metallurgical variables on the stress corrosion behavior of AISI 304 stainless steel in sodium chloride solution using the fracture mechanics approach. *Metallurgical and Materials Transactions A* **27**, 1313-1325.

Kosaki, A. (2008). Evaluation method of corrosion lifetime of conventional stainless steel canister under oceanic air environment. *Nuclear Engineering and Design* **238**, 1233-1240.

Kuniya, J., Masaoka, I. and Sasaki, R. (1988). Effect of cold work on the stress corrosion cracking of nonsensitized AISI 304 stainless steel in high-temperature oxygenated water. *Corrosion* **44**, 21-28.

Mahmoudi, A., Hossain, S., Truman, C., Smith, D. and Pavier, M. (2009). A new procedure to measure near yield residual stresses using the deep hole drilling technique. *Experimental Mechanics* **49**, 595-604.

Mahmoudi, A., Truman, C., Smith, D. and Pavier, M. (2011). The effect of plasticity on the ability of the deep hole drilling technique to measure axisymmetric residual stress. *International Journal of Mechanical Sciences* **53**, 978-988.

Mintz, T. S., Caseres, L., He, X., Dante, J., Oberson, G., Dunn, D. S. and Ahn, T. (2012). Atmospheric Salt Fog Testing to Evaluate Chloride-Induced Stress Corrosion Cracking of Type 304 Stainless Steel. *Corrosion 2012*. Salt Lake City, March 11-15: NACE.

Nakayama, G. (2006). Atmospheric stress corrosion cracking (ASCC) susceptibility of stainless alloys for metallic containers. In: VanIseghem, P. (ed.) *Scientific Basis for Nuclear Waste Management XXIX*, pp. 845-852.

Nakayama, G. and Sakakibara, Y. (2013). Prediction Model for Atmospheric Stress Corrosion Cracking of Stainless Steel. *ECS Transactions* **50**, 303-311.

NRC. (2012a). *Identification and Prioritization of the Technical Information Needs Affecting Potential Regulation of Extended Storage and Transportation of Spent Nuclear Fuel. Draft for comment.* Washington, D.C. U.S. NRC.

NRC. (2012b). *Potential Chloride Induced Stress Corrosion Cracking of Austenitic Stainless Steel and Maintenance of Dry Cask Storage System Canisters*, NRC Information Notice 2012-20, November 14, 2012. Washington, D.C. U.S. NRC.

NRC. (2013). *Finite Element Analysis of Weld Residual Stresses in Austenitic Stainless Steel Dry Cask Storage System Canisters*, NRC Technical Letter Report (ADAMS ML13330A512). Washington D.C. Nuclear Regulatory Commission.

NWTRB. (2010a). *Evaluation of the Technical Basis for Extended Dry Storage and Transportation of Used Nuclear Fuel*. NWTRB.

NWTRB. (2010b). *Evaluation of the technical basis for extended dry storage and transportation of used nuclear fuel*. Arlington, VA. Nuclear Waste Technical Review Board.

Pacific Nuclear Fuel Services, I. (1991). *Topical Report for the NUTECH Horizontal Modular Storage System for Irradiated Nuclear Fuel NUHOMS-24P*, Document NUH-002 Rev. 2A, April 1991. Adams ML110730769.

Parrott, R. and Pitts, H. (2011). *Chloride stress corrosion cracking in austenitic stainless steel: Assessing susceptibility and structural integrity*. U.K. Health and Safety Executive.

Peguet, L., Malki, B. and Baroux, B. (2007). Influence of cold working on the pitting corrosion resistance of stainless steels. *Corrosion Science* **49**, 1933-1948.

Prosek, T., Iversen, A. and Taxén, C. (2009). Low temperature stress corrosion cracking of stainless steels in the atmosphere in presence of chloride deposits. *Corrosion* **65**, 105-117.

Prosek, T., Le Gac, A., Thierry, D., Le Manchet, S., Lojewski, C., Fanica, A., Johansson, E., Canderyd, C., Dupoiron, F. and Snauwaert, T. (2014). Low temperature stress corrosion cracking of austenitic and duplex stainless steels under chloride deposits. *Corrosion*.

Scully, J. R. (1995). Electrochemical Tests. In: Baboian, R. (ed.) *Corrosion Tests and Standards: Application and Interpretation. ASTM manual series, MNL-20*. West Conshohocken, PA. ASTM International.

Tani, J. I., Mayuzurmi, M. and Hara, N. (2009). Initiation and propagation of stress corrosion cracking of stainless steel canister for concrete cask storage of spent nuclear fuel. *Corrosion* **65**, 187-194.

Turnbull, A., Mingard, K., Lord, J., Roebuck, B., Tice, D., Mottershead, K., Fairweather, N. and Bradbury, A. (2011). Sensitivity of stress corrosion cracking of stainless steel to surface machining and grinding procedure. *Corrosion Science* **53**, 3398-3415.